

Deformation history of the Yaounde Group in the Awaé - Ayos area (South-ern-Cameroon): Evidence for Pan-African thrust tectonics

OLINGA J. B.^{1*}, MINYEM, D.², MPESSE, J. E.³, EKODECK, G. E.²

¹Institut de Recherches Géologiques et Minières (IRGM), B. P. 4110, Yaoundé

²Département des Sciences de la terre, Université de Yaoundé I, B. P. 812, Yaoundé

³Département des Sciences de la terre, Université de Douala, B. P. 24157, Douala

ABSTRACT

Geological mapping and petro-structural analysis of the rocks of the Yaounde Group in the Awaé - Ayos area reveal that they experienced at least four successive deformation phases (D_1 , D_2 , D_3 and D_4). Thrusting of these rocks above the Congo craton happened during the D_2 and D_3 phases. Structural features related these phases (flat lying foliations and shear bands, S-C fabrics, abundant asymmetric folds, asymmetric boudinage and porphyroblasts) suggest that: (1) strain results from large-scale horizontal shearing deformation in a non coaxial regime; (2) the regional stretching/mineral lineation represents the direction of transport; (3) the thrusting probably took place west to south-westwards. The D_3 phase was later followed by the development of dextral strike slip shear zones and large scale N-S to NE-SW directed folding related to the D_4 phase. This structural evolution show clear similarities with the one observed in the metasediments of the Mintom area, and therefore allow considering all these formations as a single allochthonous structural unit thrust onto the Congo Craton.

Key words: Awaé - Ayos; Yaounde Group; thrust tectonics; non coaxial regime; allochthonous structural unit.

RESUME

L'analyse pétro-structurale détaillée des formations géologiques du Groupe de Yaoundé, dans la région d'Awaé - Ayos, met en évidence l'existence d'une déformation polyphasée (D_1 , D_2 , D_3 et D_4). Les phases D_2 et D_3 correspondent au charriage de la nappe de Yaoundé sur un autochtone archéen (craton du Congo). Les éléments structuraux associés à ces deux phases de déformation (cisaillements plats, foliation subhorizontale, linéation minérale et d'étirement, plans "C" et "S", plis et porphyroblastes dissymétriques) suggèrent que: (1) la déformation majeure est contrôlée par des cisaillements sub-horizontaux en régime non coaxial; (2) la linéation régionale correspond à la direction de transport; (3) ces roches ont été impliquées dans une tectonique tangentielle majeure vers l'Ouest ou le Sud-Ouest. La phase D_4 correspond à des cisaillements dextres de direction moyenne $N80^\circ E$, associés à des mégaplis de direction N-S à NE-SW. Ces différents traits structuraux s'apparentent à ceux observés plus au Sud dans les métasédiments de Mintom. Ces formations représentent probablement une même unité structurale allochthone, charriée sur le craton congolais.

Mots-clés : Awaé - Ayos; Groupe de Yaoundé; tectonique tangentielle; regime non coaxiale; unité structurale allochthone.

INTRODUCTION

The Congo craton, ca. 2.8 Ga old (Lasserre et Soba, 1979; Toteu et al., 1994), is one of the main tectonically significant features of the Precambrian crust in Southern-Cameroon. It is delimited to the north by the Neoproterozoic Fold Belt of Cameroon (NFBC; 620 + 10 Ma; Penaye et al., 1993; Penaye et al., 2004) underlying the central and northern part of the country (Fig. 1a). Its northward extension beyond the Yaounde town and beneath the NFBC is evidenced by a steeply dipping intracratonic fault that cross-cut the NFBC - Congo craton gently dipping contact (Manguelle Dicoum et al., 1992). The NFBC in the Awae - Ayos area (Fig. 1b, 1c) comprises three main rock units of

varying metamorphic grade (Olinga, 2003): (i) various medium to high-grade gneisses and micaschists (most of which are migmatized), (ii) interlayered amphibolites and metamorphosed calc-alkaline intrusive rocks, (iii) low grade schists and quartzites (Ayos series). Detailed descriptions of the chemical and petrographic characteristics of these rock units are provided by Olinga, (2003). They are thought to be derived from epicontinental deposits on the northern edge of the Congo craton, which were intruded by dioritic rocks in either a continental basin or a passive margin environment (Nzenti, 1988; Olinga, 2003). These rocks have accordingly undergone different phases of deformation as evidenced by different types of

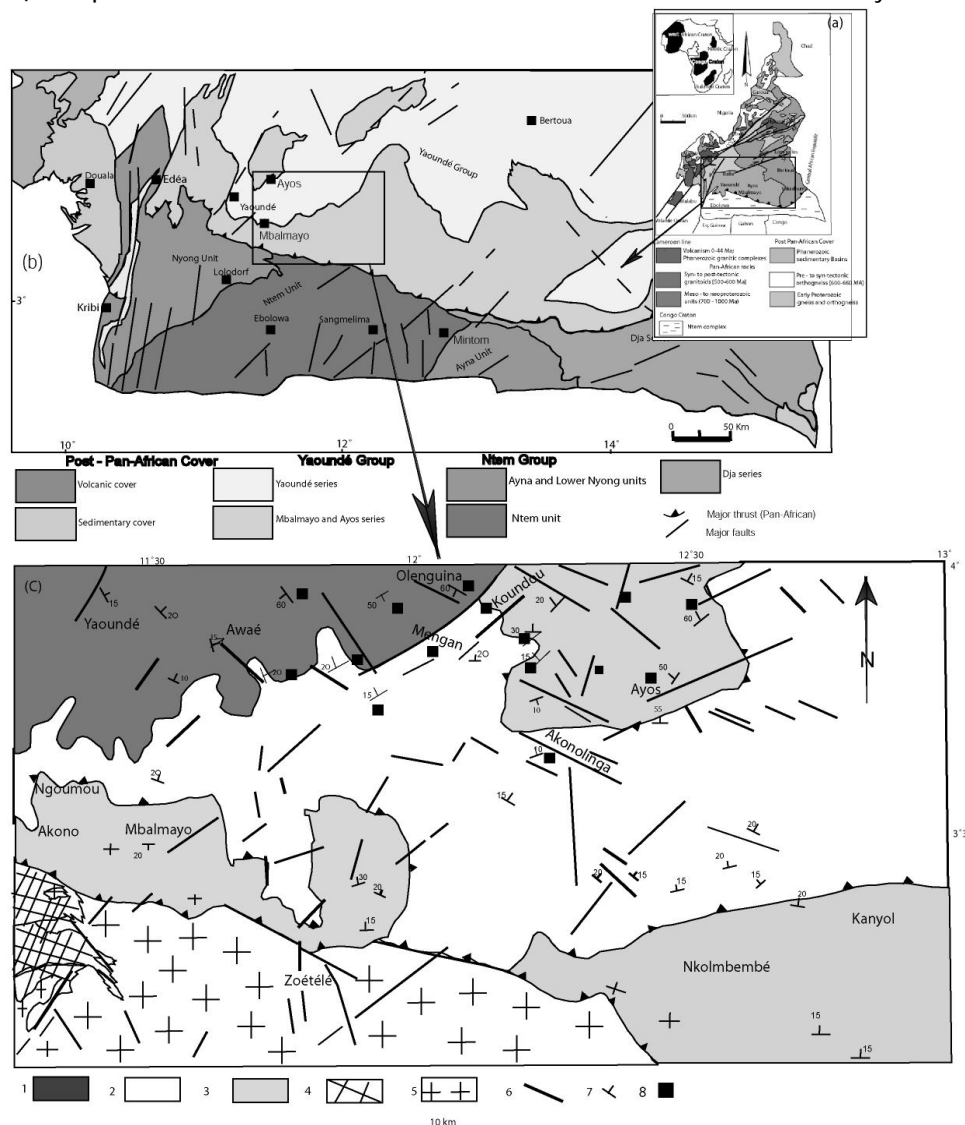


Fig. 1: (a) Location of Southern - Cameroon within the simplified geological sketch map of Cameroon (modified from Soba, 1989); (b) Simplified geological sketch map of southern Cameroon (modified from Maurizot, 1986) showing the main geological units, and location of the Awae - Ayos; (c) Geological map of the Awae - Ayos and neighbouring areas (modified from Champetier de Ribes and Aubague, 1956; Maurizot, 1986; Olinga 2003) showing location of studied outcrops; Legend as follow: Pan-African units: 1- micaschist; 2 - high grade gneiss; 3- low grade schists; 4- Paleoproterozoic units (lower Nyong series); 5- Archean basement (Ntem complex); 6- faults; 7- strike and dip of foliation; 8 location of studied outcrops

Table 1: Representative biotite analyses of the high grade gneisses and micaschists of the awaé area.

Kyanite – garnet gneisses of Top			Biotite – muscovite micaschists of Olenguina					
Sample	T2B1	T2B2	OL1B6	OL1B3	OL1B4	OL3B2	OL3B5	OL3B8
SiO ₂	37.15	39.74	36.7	47.08	46.57	47.07	36.79	35.81
TiO ₂	2.13	2.09	3.08	1.5	0.84	1.5	3.26	2.54
Al ₂ O ₃	18.16	18.58	17.52	35.36	35.79	34.56	18.08	17.85
FeO	13.1	11.8	15.9	2.39	2.5	2.6	16.5	16.2
MnO	0.01	0.03	0.02	0.01	0.05	0.01	0.01	0.03
MgO	16.57	15.46	13.31	1.48	1.25	1.46	13.18	13.55
CaO	0.01	0.03	0.01	0.02	0.01	0.03	0.02	0.03
Na ₂ O	0.32	0.33	0.16	0.42	0.58	0.51	0.18	0.16
K ₂ O	9.28	9.35	9.66	8.42	9.78	9.37	9.58	8.95
Total	97.71	97.5	96.36	97.68	97.34	97.1	97.56	95.14
Ti	0.236	0.226	0.348	0.148	0.083	0.148	0.364	0.29
K	1.724	1.718	1.851	1.406	1.638	1.57	1.814	1.736
Na	0.091	0.092	0.047	0.106	0.148	1.13	0.052	0.047
Mn	0.001	0.004	0.002	0.001	0.005	0.001	0.001	0.004
Ca	0.002	0.005	0.002	0.003	0.001	0.004	0.003	0.005
Mg	3.635	3.319	2.98	0.289	0.244	0.286	2.917	3.071
Fe ₂	1.61	1.42	2.001	1.52	0.165	1.176	2.044	2.063
Si	5.32	5.57	5.35	6.16	6.1	6.18	5.31	5.29
Al ^{IV}	3.15	3.15	3.1	5.45	5.53	5.34	3.16	3.19

structural features which range from asymmetrical folds and boudinage, foliations, shear bands and rotated porphyroblasts. This paper is therefore aimed at using field geological mapping and petro-structural analyses to reconstitute the deformation history of the Yaounde Group and discuss a model for its structural and metamorphic evolution.

2.0 MATERIAL AND METHODS

The study combines field and analytical work both performed to achieve the specific aims mentioned above. The item used for the field study is the classical mapping equipment. Petrographic study was carried out on selected thin sections, using polarizing microscope. Mineral analyses (tables 1 and 2) were done

Table 2: Representative garnet analyses of the high grade gneisses and micaschists of the awaé area.

Kyanite – garnet gneisses of Top			Biotite – muscovite micaschists of Olenguina					
Sample	T2G1	T2G2	OL1G10	OL1G15	OL1G3	OL3G11	OL3G9	OL3G2
SiO ₂	37.68	37.28	36.94	37.26	37.92	36.06	36.78	37.7
TiO ₂	0.03	0.03	0.01	0.06	0.01	0.01	0.05	0.03
Al ₂ O ₃	21.02	21.61	20.16	21.29	21.11	21.78	20.6	21.31
FeO	28.9	27.7	30.6	31.4	30.5	31.2	30.9	30.8
MnO	1.34	1.3	1.24	1.35	1.2	1.22	1.22	1.28
MgO	8.76	8.47	5.71	4.49	4.88	4.67	5.46	4.86
CaO	2.16	2.9	4.56	3.68	4.2	4.49	4.71	3.74
Na ₂ O	0.03	0.03	0.02	0.02	0.02	0.01	0.01	0.03
K ₂ O	0	0	0	0	0	0	0	0
Total	99.89	99.36	99.21	99.55	99.79	99.43	99.71	99.79
Ti	0.002	0.002	0	0.004	0	0.001	0.003	0.002
K	0	0	0	0	0	0	0	0
Na	0.004	0.004	0.003	0.003	0.003	0.002	0.002	0.005
Mn	0.089	0.086	0.084	0.091	0.08	0.083	0.083	0.086
Ca	0.181	0.244	0.392	0.315	0.356	0.386	0.403	0.318
Mg	1.022	0.991	0.684	0.534	0.576	0.558	0.65	0.575
Fe ₂	1.891	1.821	2.052	2.096	2.018	2.093	2.065	2.046
Si	2.951	2.926	2.964	2.975	3.005	2.894	2.940	2.99
Al	1.94	1.99	1.90	2.00	1.97	2.06	1.94	1.99

on four selected samples using a Cameca SX-50 electron microprobe (University of Tuebingen, Germany); the acceleration voltage was 15Kv, with a sample current and beam diameter of 10nA and 2µm, respectively; the counting time was 10 sec. Field work was focused on lithological and structural description in order to draw a field map and define metamorphic and structural units. The widespread forest and lateritic cover in the study area dictate that the examination of rocks be limited to more or less extended outcrops along quarries, roads, inselberg reliefs or flagstones (Fig.

1c). Analytical work was focused on the reconstruction of different phases of shearing, folding, and metamorphism along the study area using the field map, the petro-structural and mineralogical data. Structural overprinting relationships, deformation styles, structural orientations and relations between deformation and crystallisation were helpful indicators. Statistical methods (e. g. equal area stereographic representation) were used to determine the orientation in space and the kinematic evolution of structures related to each deformation phase.

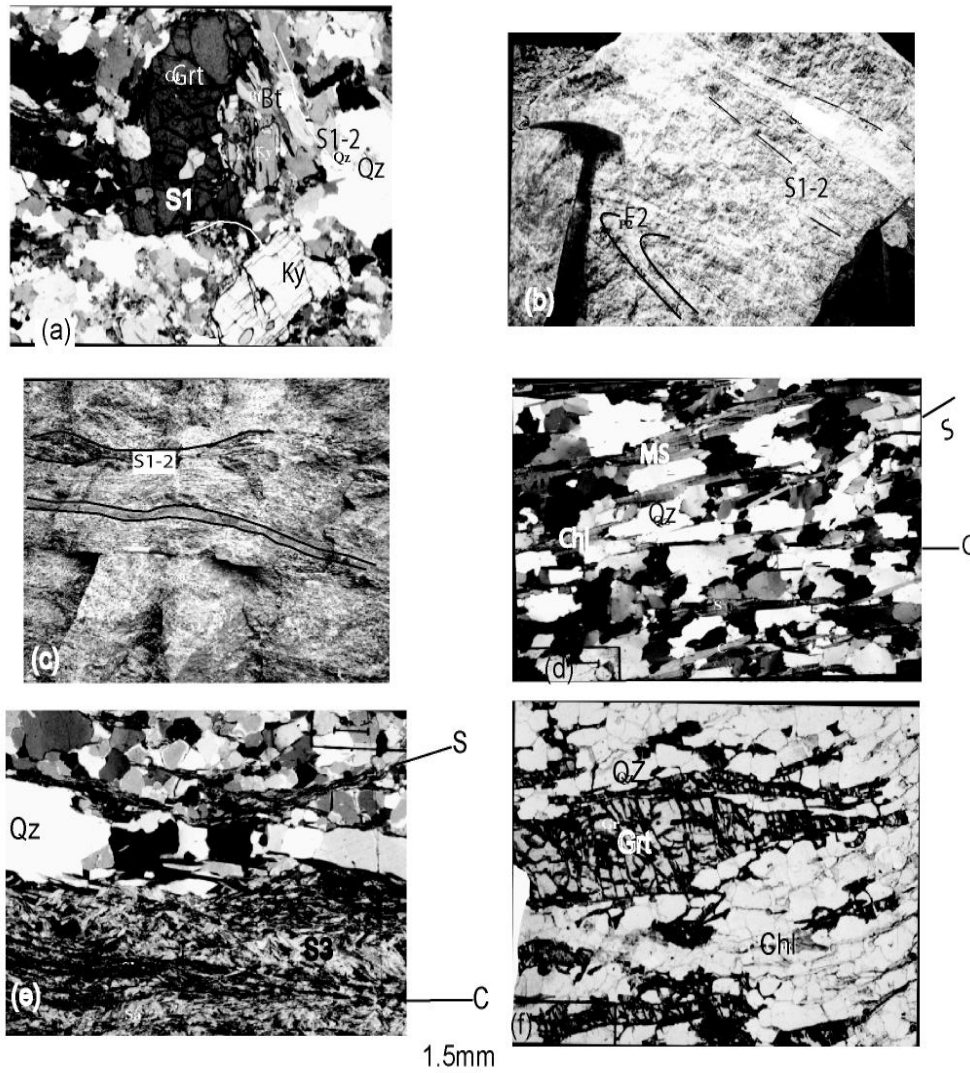


Fig. 2: Microfabrics and fabrics of the Awaé-Ayos rocks. (a) Photomicrographs showing gneisses of the Top area under crossed nicols; the main foliation (S2) is underlined by more or less elongated crystals of Qtz + Bt + Ky + Rt + Gr + Kfs; garnet occurs as rounded porphyroblast wrapped around by the main foliation; (b) Photograph of a quartzo-feldspathic vein displaying F2 isoclinal and S1-2 axial planar foliation; the occurrence of S1 is restricted to the F2 fold hinge (Ky-grt bearing gneiss; Top quarry, east of Awaé). (c) Photograph showing boudinaged a garnet - amphibole gneiss interlayered in a garnet and kyanite - gneiss (Top quarry, east of Awaé); (d) Microphotographs of the Koundou area (east of Awaé) showing muscovite bearing quartzites; the main S3 schistosity displays C/S fabrics related to D3 thrusting deformation; quartz is observed as elongated new grain or as polycrystalline ribbons with uniform extinction; (e) and (f) Microphotographs of the ayos area Phyllonitic foliation S3/4 in (a) achlorite schists (b) garnet bearing quartzites; this foliation displays C/S fabrics, quartz and garnet ribbons with a very fine grained matrix and contains large amounts of chlorite and muscovite and small amount of sericite and biotite.

3.0 RESULTS AND INTERPRETATION

3.1 *The main petrographic units of the Awaé-Ayos area*

Mineral abbreviations in the text, tables and figures are those of Kretz (1983).

3.1.1 *Medium to high-grade gneisses and micaschists*

This group mainly consists of kyanite - garnet gneisses and biotite-muscovite-garnet micaschists; quartzite and basic rocks are observed as discontinuous layers within these main rocks.

The Ky-Grt gneisses are the most abundant metamorphic rocks in the Awaé area; the best outcrops are found around Ayene, Top and Ngona villages (Fig. 1c). They are coarse- to medium-grained mesocratic gneisses and display a granolepidoblastic textures (Fig. 2a). Compositional layering defined by variations in modal proportions of biotite with respect to the felsic minerals, is present on a centimetre scale. This compositional layering is enhanced through migmatization, and is parallel to the metamorphic tectonite fabric defined by oriented biotite and kyanite. Their main mineral assemblage consists of variable amounts of quartz (20 - 25 vol. %), biotite (15 - 20 vol. %), perthitic K-feldspar (5 - 10 vol. %), garnet (5 - 10 vol. %), kyanite (5 - 10 vol. %), plagioclase An₂₀₋₃₀ (5 - 10 vol. %), rutile (1 - 3 vol. %), sillimanite (<1 vol. %); accessories are zircon and graphite; retrograde phases are epidote, chlorite and biotite. These gneisses are intensively migmatized, as demonstrated by quartzofeldspathic veins which run parallel to, or cross-cut the banding of the rocks. Migmatites formed by partial melting of Ky-Grt gneisses exhibit a well-pronounced layering marked by leucosome bands and cross-cut by several generations of mobilizates (Fig. 2b). Leucocratic layers are made up of quartz, plagioclase (An₃₀₋₃₈) and potassic feldspar, including sometimes garnet grains and biotite flakes; patch and string perthites are most common; graphic intergrowths of quartz and alkali feldspar (myrmekites) are observed in some samples. Leucosome bands sometimes display garnet crystal patches surrounded by relicts of biotite. In some samples, the symmetrical arrangement of biotite rich layer on either side of these bands indicates that the migmatization resulted from in situ partial melting. Melanocratic layers contain biotite flakes parallel to the main foliation and rounded garnets with inclusion of rutile, biotite, graphite and quartz. Accessory minerals are apatite and zircon.

The Bt-Musc-Grt bearing micaschists are confined in Olenguina and Akomkada areas (Fig. 1c). They are fine-

to medium-grained mesocratic rocks, exhibiting a pronounced penetrative cleavage (generally made up of planar orientation of biotite and muscovite) and a granolepidoblastic texture. Their main mineral assemblage is made up of quartz (20 - 35 vol. %), biotite (15 - 25 vol. %), muscovite (10 - 15 vol. %), plagioclase An₂₀₋₂₅ (10 - 15 vol. %), garnet (5 - 10 vol. %), kyanite (3 - 5 vol. %), accessories are zircon and graphite; secondary phases are scarce chlorite flakes and epidote. In both gneisses and micaschists, quartz aggregates display subgrains with undulatory extinction and small elongated new grains; a beginning of ribbon like organisation can also be observed. Garnet normally occurs as rounded porphyroblasts moulded by the main foliation, with quartz, biotite and graphite as inclusions, the latter sometimes oriented at high angle with respect to the compositional layering of the rock, which suggests early growth with respect to the prevailing structure. Compositionally, these garnets are of almandine-pyrope series with small amount of spessartine and grossular (table 2). Some of them display two growth zones: inclusion-free rims (Grt₂) and cores with quartz, biotite and graphite as inclusions (Grt₁). Biotite occurs either as small crystals interstitial to garnet suggesting a retrograde origin or as primary flakes oriented parallel to the main foliation. Primary biotites are characterised by high Ti contents (cation average $0.16 < Ti < 0.35$, [O=24]; table 1) which is a common feature in granulite facies environments (Dymek, 1983). Sillimanite is found as small secondary needles (fibrolite) in some of these rocks.

3.1.2 *Metamorphosed basic rocks*

The metamorphosed basic rocks are mainly made up of Bt-Grt amphibolites and Bt-rich rocks; they often occur as intruded or interlayered boudinaged bodies in metasedimentary rocks (Fig. 2c).

Bt-Grt amphibolites are the dominant rock type; they are dark coloured granoblastic rocks displaying a weak foliation. They are composed of hornblende (25 - 35 vol %), biotite (20 - 25 vol %), plagioclase An₃₀₋₃₅ (10 - 15 vol %), quartz (10 - 15 vol %), garnet (5 - 10 vol %) and clinopyroxene (1 - 5 vol %); accessories are sphene, magnetite, and zircon. The garnet normally occurs as rounded crystals displaying an inclusion-free rim (Grt₂) and a core with quartz, biotite and plagioclase as inclusions (Grt₁). The biotite occurs as small flakes between quartz, plagioclase and hornblende. Hornblende porphyroblasts are poikiloblastic, displaying inclusions of pyroxene and quartz.

Bt-rich gneisses appear as dark-grey, fine- to medium-grained rocks. They are predominantly composed of biotite (60-70% vol.), quartz (5-10% vol.), plagioclase (5 - 10 % vol.) and garnet (<5%); accessories are apatite and zircon.

3.1.3 Low-grade schists and quartzites

Schists and quartzites are surrounded by gneisses and micaschists (Fig. 1c). They are fine-grained in texture, and greenish in colour.

Quartzites can be seen either as a mapable rock unit (Koundou area) or as lenses interlayered in garnet-chlorite schists (Ayos area). In these quartzites, cleavage is strongly developed, displaying alternating millimetre thick muscovite rich and quartz rich layers (Fig. 2d). They are composed of quartz (50 - 65 vol %), muscovite (10 - 15 vol %), chlorite (5 - 10 vol %) and orthoclase (1.5 vol %); tourmaline and opaques are also present. Muscovite and chlorite occur mainly in two textural habits: (i) schistosity defining flakes overgrown by large euhedral megacrysts; and (ii) C/S structures.

Schists display a centimetric compositional cleavage with alternating chlorite - muscovite rich and quartz rich layers (Fig. 2e). They are composed of quartz (20 - 30 vol %), chlorite (20 - 25 vol %), muscovite (15 - 20 vol %), garnet (5 - 10 vol %), sericite (1 - 5 vol %), opaques (1 - 3 vol %) and orthoclase (1.5 vol %); accessories are calcite, biotite, epidote, tourmaline and apatite. Garnets are observed in large blasts of 1-10mm size showing quartz, muscovite and opaque as inclusions (Fig. 2f). Compositionally these garnets are of almandine- spessartine and grossular series with small amount of pyrope (olinga, 2003). Biotite is scarce and occurs as very small flakes included in chlorite, suggesting that biotite provides a favourable site for chlorite nucleation. The whole rock appears as

phyllonites displaying inequigranular quartz ribbons with a very fine grained matrix, containing large amounts of chlorite and muscovite and small amounts of sericite and biotite (Fig. 2e, 2f). In both schists and quartzites, secondary quartz and chlorite display large undeformed crystals, with muscovite as the most common inclusion in quartz.

3.2 Deformation history and phases assemblages

The Pan-African event produced intense deformation and metamorphism in the Awae - Ayos rock units. At least four main deformation phases (D_1 , D_2 , D_3 and D_4) are recognised, based on overprinting relationships, deformation styles and structural orientations. In addition, a pre-metamorphic compositional layering (S_0) is identified in some rocks.

3.2.1 D_1 structures

The first deformation phase D_1 predated development of the dominant foliation; the earliest foliation (S_1) related to this event is isoclinally folded and a second planar foliation (S_2) appears. Thus, S_1 foliation is completely transposed and commonly parallel to the dominant foliation (S_2); it can only be differentiated in the F2 fold hinges. In both gneisses and micaschists, D_1 is also manifested as helicitic inclusions of opaque + quartz + kyanite + rutile + biotite \pm plagioclase (gneisses and micaschists) and biotite + plagioclase + quartz (amphibolite) in garnet porphyroblast cores (Fig. 2a). The D_1 phase is therefore associated with remnants of early upper amphibolite or granulite facies metamorphism. No conspicuous regional movement direction has been observed for D_1 .

3.2.2 D_2 structures

The dominant E-W to NE-SW trending structures of the Awae-Ayos rock units are the result of the second deformation phase (D_2); the latter mainly affects high grade gneisses and micaschists; it is characterized by:

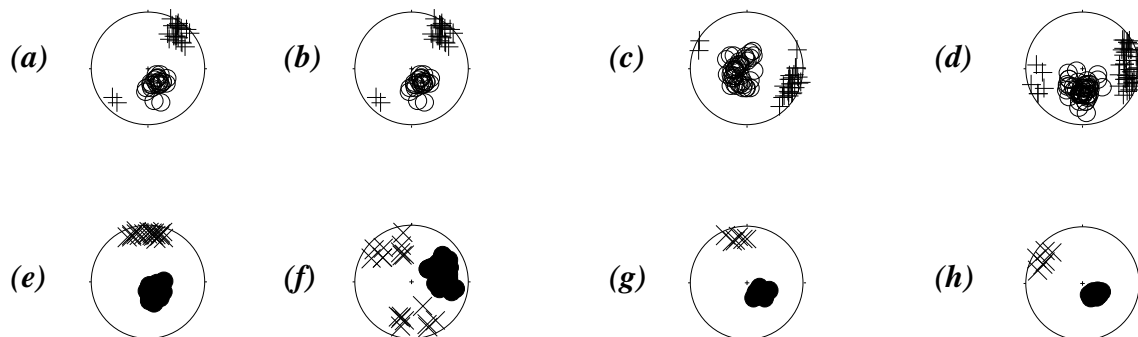


Fig. 3: Lower - hemisphere equal - area representation of the foliations and lineations: S2 foliation (empty circles); L2 lineation (+ crosses); data from: Ebassi (a), Nkomban (b) and Top (c). S3 foliation (black circles); L3 lineation (x crosses); data from Koundou (e), Ayene (f), Akonolinga (g) and (h).

(1) a flat-lying foliation, S_2 , which strikes $N80^\circ - 100^\circ E$, and dips gently ($15^\circ - 20^\circ$) to the north or the south (Figs. 2a, 2b, 2c; 3a, 3b, 3c); (2) an associated strong stretching / mineral lineation, L_2 , defined by stretched quartz aggregates, elongated feldspars, and shape preferred alignment of kyanite crystals, that plunges gently and trends to the West ($N80-100E/25$; Figs. 3a, 3b, 3c); (3) mesoscopic flat-lying ductile shear bands (C_2) which have an average dip of $20^\circ - 25^\circ$ and a top to the west or south-west sense of shear (Figs. 4a, 4b). The S_2 foliation is axial planar to F_2 asymmetrical isoclinal folds (Figs. 2b, 3b) which show a consistent vergence toward west or south - west (Fig. 3b); their axes plot close to the maximum of the stretching lineation. Eye structures are common (Fig. 4c); these structures are judged to be dominantly sheath folds; consequently finite strain is very intense. In the migmatitic rocks, ptygmatic folds and asymmetric en echelon folds with thickened hinges and thinned limbs are observed. Some garnets which grew synkinematically with respect to D_2 structures display asymmetric pressure shadows (Fig. 2a). The M_2 mineral assemblages occur mainly as sub-automorphic crystals oriented along the S_2 foliation or the C_2 shear planes, or defining the L_2 lineation. It includes: (1) quartz + garnet + plagioclase + kyanite

+ rutile + biotite in high grade gneisses (Fig. 2a) and micaschists; (2) quartz + garnet + plagioclase + clinopyroxene + hornblende \pm biotite in biotite-garnet amphibolites. This appears to indicate that D_2 occurred under upper amphibolite or granulite facies metamorphic conditions.

3.2.3 D_3 structures

The feature distinguished by the S_2 foliation defines a regional scale fold pattern (F_3) which has sigmoidal forms, trends NE-SW and verges easterly (Fig. 6). The folding of the syn- D_2 nappe is induced by its N-S shortening during the D_3 event. In high grade gneisses and micaschists the following structures are co-eval with the F_3 folding: a strong crenulation cleavage (S_3) oblique to the C_2/S_2 planes (Fig. 4d). In low grade schists and quartzites, prominent features coeval with the D_3 event are: (i) a flat lying mylonitic schistosity (S_3) exhibiting S-C fabrics and striking $N100 - 80^\circ E$ (Figs. 2d, 3e, 3f, 3g, 3h); (ii) a strong stretching lineation (L_3) which trends N-S and plunges moderately to the north or the south (Figs. 2d, 3e, 3f, 3g, 3h); this lineation is commonly observed imprinted on the S_3 foliation. All these features can be used to infer a southward displacement coeval with a N-S shortening direction of the nappe. Field

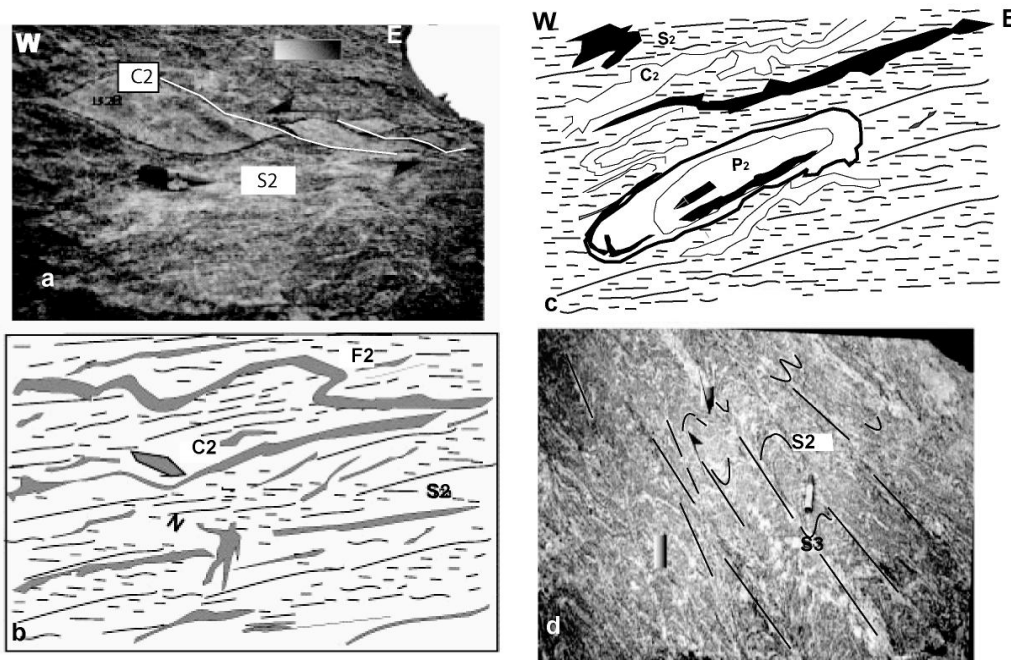


Fig. 4: Photographs of syn- D_2 structures in the Ngona and Top villages (sections XZ, where X is horizontal).
(a) E-W flat lying S_2/C_2 foliation showing asymmetrically boudinaged and laminated quartzofeldspathic layers (east of Ngona).
(b) Deformed veins in section perpendicular to the stretching lineation L_2 . Asymmetrically folded vein is induced by C_2 flat lying shear planes with a top to the west or southwest sense of movement (Top quarry).
(c) Eye structures (sheath folds) induced by C_2 flat lying shear planes;
(d) S_3 schistosity bands cutting through earlier formed foliation in the Awaé gneisses (horizontal plane).

observation indicates that schists and quartzites plunge gently to the North and lie under the high metamorphic rock group (Fig. 5). This geometrical relationship correlates with an increase of the deformation intensity from gneisses to schists and quartzites. It is marked by a widespread occurrence of C/S fabrics in schists and quartzites (Fig. 2d) and allows us to consider these rocks as the sole of a large scale nappe structure generated during the major D₂ and D₃ thrusting event. The M₃ mineral assemblages grew synkinematically with respect to D₃ structures. The lowest-grade assemblage defined by retrogressive phyllonitic schists and strongly deformed quartzites is found close to the sole thrusts, underlining C/S fabrics, the S₃ schistosity (Fig. 2d) and the L3 lineation. It includes quartz + orthoclase + muscovite + chlorite, and is often overgrown by large euhedral garnet; this indicates that in schists and quartzites, the M₃ event occurred under greenschist facies metamorphic conditions. In high grade gneisses and related migmatites, the same event occurred under amphibolite facies conditions; it is mainly composed of quartz + biotite + muscovite + fibrolite (in kyanite-garnet bearing gneisses and micaschists) or quartz + biotite + hornblende + garnet (in biotite-garnet amphibolites) underlining the S3 crenulation cleavage. These major mineral assemblages are characterised by

the widespread development of biotite and muscovite in kyanite-garnet bearing gneisses and micaschists, and the growth of hornblende and biotite at the expense of garnet and pyroxene in biotite-garnet amphibolites. This allows the the following points to be emphasised: (1) in high grade rocks, the presence of early assemblages (coeval with D₁ and D₂ phases) containing kyanite, and the development of sillimanite in the late stages (D₃ phase) are consistent with a strong decompression of the P-T path that affected the kyanite-bearing assemblages and produced muscovite-sillimanite bearing assemblages; (2) in low grade schists and quartzites, the widespread occurrence of chlorite-calcite-epidote coexisting with K-feldspars and garnet witnesses to considerable temperature decrease for the latter assemblage.

3.2.4 D₄ structures

The D₄ phase is expressed by late dextral E-W trending strike slip shear zones which folded, sheared and partly obliterated the previous structures. Two main structural features are recognised: the dextral strike slip shear zones and the large scale fold pattern (Fig. 5). The structures related to these features are restricted around Olénguina - Akomkada and AyoS areas.

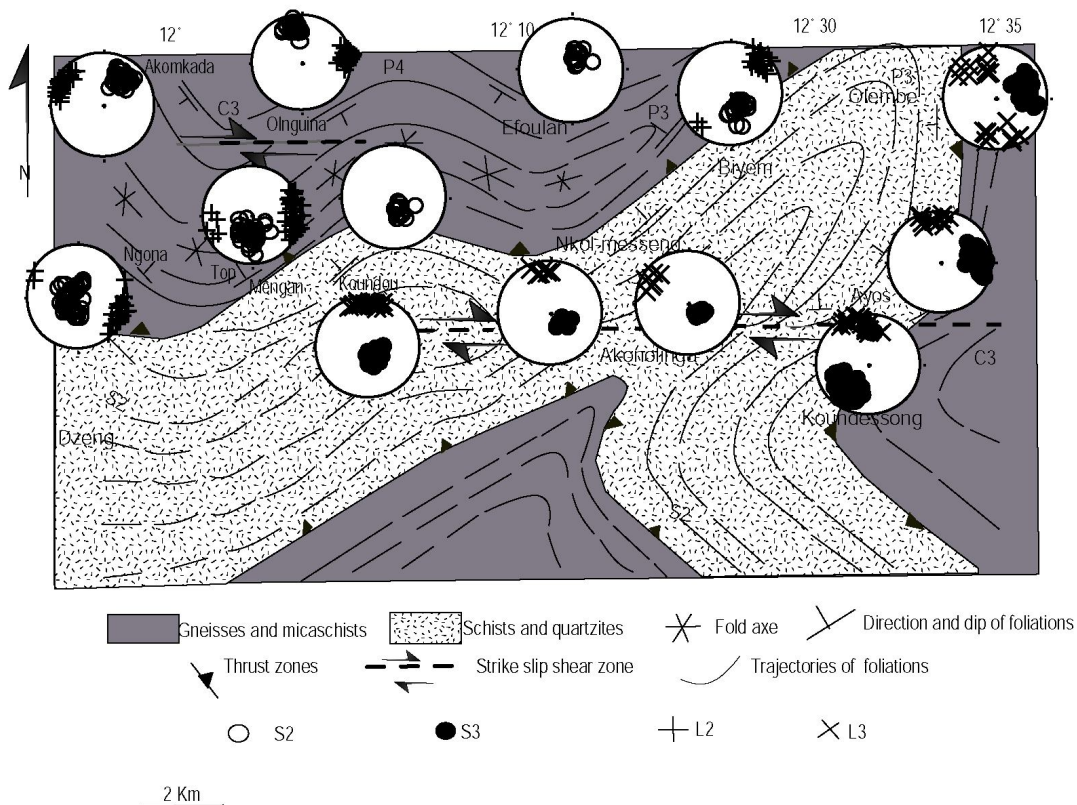


Fig. 5: Major structures of the Awae - AyoS area, showing structural domains and equal area projection to illustrate attitudes of regional folds and mylonites zones.

The dextral strike-slip shear zones produced mylonites, phyllonites and a strong stretching lineation. Phyllonites are defined by a fine grained matrix with elongated quartz and feldspar, and aligned muscovite and chlorite; most mineral grain sizes are extensively reduced by recrystallisation (Fig. 2e, 2f). In some samples, petrographic fabrics show the strong development of rotational deformation features (Fig. 6a, 6b, 6c); some garnets bear a strong sigmoidal internal schistosity (Fig. 6b). The C_4 steeply dipping shear planes (average dip N60-80S) trend N80 - 100E and bear a strong horizontal stretching lineation that also trends E-W and plunges gently (average 15°) to the W or the E (Figs. 7a, 7b, 7c, 7d). Some of these planes wrap asymmetric boudins and folds and are cross-cut by C' -type shear planes (Berthé et al, 1979). The angular relationships between these respective planes, the orientation of garnet snowball inclusions and asymmetrical folds or boudins are consistent with dextral sense of shear movement. The F_4 regional scale folds are coeval with the C_4 shearing; significant sigmoidal bending of the

F_3 folds indicates a dextral sense of shear (Fig. 6a, 6b, 6c). At the outcrop scale, D_4 produced asymmetric folds (F_4), a strong crenulation cleavage (S_4) and a crenulation lineation (L_4 ; Fig. 6d) parallel to the F_4 fold axes. The F_4 folds can commonly be differentiated from F_3 by fold interference patterns. In both gneisses and schisto-quartzitic rock units, the D_3 and D_4 structures are defined by the same mineral assemblages, suggesting that they occurred under the same metamorphic conditions (e. i. amphibolite facies for high grade gneisses and micaschists and greenschist facies for schists and quartzites).

3.3 P-T estimates

Temperature estimates in metapelitic rocks (e. i. Ky-Grt gneisses and Bt-Musc-Grt micaschists) were obtained by application of Grt-Bt thermometer (Ferry and Spear, 1978; Perchuk and Lavrent'eva, 1981; Hodges et Spear, 1982; Ganguly and Saxena, 1984; Indares and Martingole, 1985a; Indares and Martingole, 1985b). In order to avoid erroneous temperatures, the

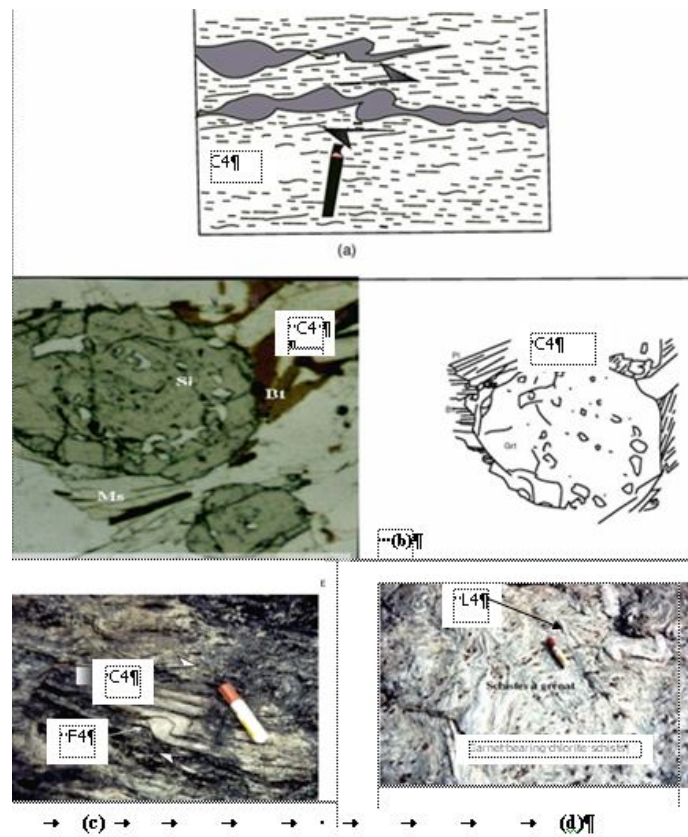


Fig. 6: Structures related to C_4 ductile strike slip shear zone in Awaé and Ayos areas (horizontal plane).
(a): Photograph of a quartzofeldspathic vein asymmetrically folded during D_4 phase, indicating a dextral strike slip shear (Olenguina area).
(b) Microphotograph of snow-ball quartz inclusions at the core of a garnet porphyroblast indicate a shear movement (micaschists; Olenguina area).
(c) Photograph of folded and stretched quartz veins showing dextral strike slip shear (schists; Ayos area).
(d) Photograph of crenulation lineation (L_4) parallel to the F_4 fold axes (schists; Ayos area).

calculations of Hodges and Spear, (1982), and Ganguly and Saxena, (1984), which are both based on four components mixing models for garnet solid solutions, and which are therefore universally applicable, were chosen. Core-rim thermobarometry has been used by many workers to construct P-T paths in granulite terrains (e. g. Bohlen et al., 1987); we used this, applying Grt-Bt thermometry, to garnet rimmed by biotite + muscovite coronas. To obtain peak temperatures, we used the analyses from the inner parts of garnet porphyroblasts, whereas rims were used to determine the retrograde metamorphic conditions. The results of these calculations are summarized in tables 3 and Fig 8. The calculated temperatures yield results in the range of 620-760°C; the peak conditions obtained from core garnet vs. matrix biotite may therefore be estimated at $760 \pm 50^\circ\text{C}$. The presence of rutile and kyanite in syn- D_1 and D_2 mineral assemblages indicates that very high pressure conditions were attained during these stages. The stability of kyanite at temperatures higher than 750°C is consistent with the stability of Garnet + clinopyroxenes assemblage in basic rocks and indicates pressure higher than 9 Kb (Thompson and Algor, 1977; Spear, 1993). The pressures and temperatures required for the syn- D_1 and D_2 mineral assemblages can hence be roughly estimated at $> 760^\circ\text{C}$, and $> 9\text{KB}$.

4.0 DISCUSSION

The petro-structural analysis of the Yaounde Group in the Awaé-Ayos area show at least four main tectonic

and metamorphic phases (D_1 , D_2 , D_3 and D_4); deforming conditions are ductile to brittle-ductile. The tectonic significance of the D_1 event is unknown. Early works (Ball et al., 1984, Jegouzo, 1984, Nédélec et al., 1986, Toteu et al., 1987, Nzenti et al., 1988; Ngako et al., 2003, Toteu et al., 2006) on the Yaounde group reveal that during the D_2 phase, these rocks suffered a main thrust tectonics under peak conditions of granulite facies metamorphism, which later evolved under medium- to low-grade metamorphic conditions. This interpretation was questioned by Mvondo et al., (2003), Mvondo et al., (2007a) and Mvondo et al., (2007b) who argued that: (i) the stretching lineation in the Yaounde Group does not represent the transport direction as it is imprinted on non mylonitic flat lying foliation; (ii) there is no evidence attesting that the edge of the Congo craton suffered collision tectonics; and (iii) the allochthonous position of the Yaounde Group over the Congo craton has not been proved. These authors proposed for the D_2 phase deformation, a double ductile extensional model based on major N-S and minor E-W trending structures. However, detailed mapping of the structures related to the second and third deformation phases in the Awaé - Ayos area allow to trace large scale sheeted rock units with a top to the west or south-west displacement. Thrust tectonics indicators (flat lying foliations and shear bands, stretching lineation, S-C fabrics, abundant asymmetric folds, asymmetric boudinage and porphyroblasts) suggest that: (i) strain results from large-scale horizontal shearing deformation in a non coaxial regime; (ii) the

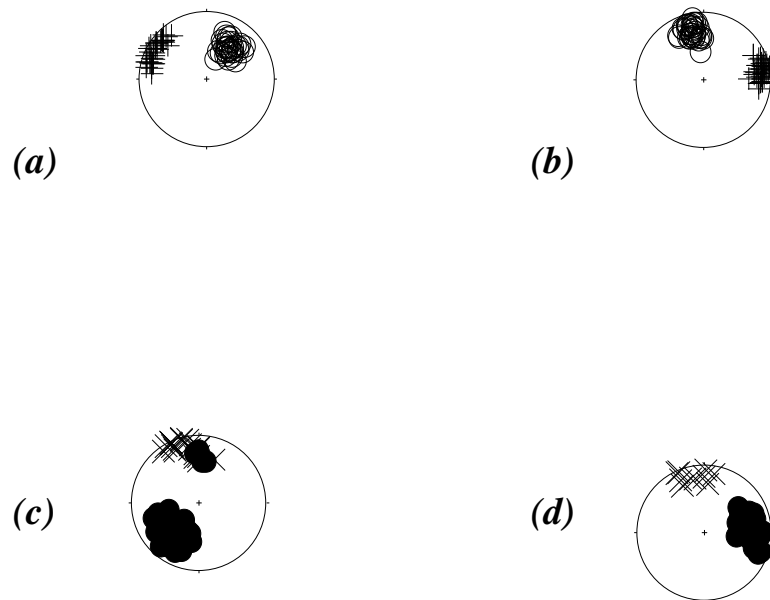


Fig. 7: Lower - hemisphere, equal - area representations of fabric data from Awaé - Ayos strike slip shear zones features (D_4). The data display the relationship between C_4 planes (circles) and L_4 lineation (crosses): subhorizontal lineation lies in the C_4 subvertical planes. **(a)** Plot from the Akomkada area (micaschists). **(b)** Plot from the Olenguina area (micaschists). **(c)** Plot from the Akokmekka area (schists); **(d)** Plot from the Ayos area (schists).

Table 3: Summary of temperature estimates from Hodges and Spear (1982) calibrations of the garnet - biotite thermometer.

Sample – rock type	Garnet			Biotite			Temp (°C)
	X _{Fe}	X _{Ca}	X _{Mn}	X _{Fe}	X _{Ti}	X _{Al}	
OL1 (micaschists; rim)	0.83	0.02	0.03	0.48	0.07	0.14	622
T2 (gneiss; rim)	0.79	0.03	0.02	0.43	0.10	0.07	657
T2 (gneiss; core)	0.76	0.02	0.01	0.43	0.11	0.05	780
OL1 (micaschists; core)	0.81	0.02	0.07	0.52	0.09	0.11	766

deformation mechanism has involved heterogenous simple shear of an originally flat lying rock unit (given the fact that sub-horizontal stretching lineations are sub-parallel to axes of asymmetrical and sheath folds); (iii) the regional stretching lineation represents the direction of the shearing and transport (as it is often imprinted on strongly deformed flat lying planes); (iv) thrusting probably took place west to south-southwestwards. According to Penaye et al., (1993), the plutonism in the Yaounde Group was interrupted during the the D2 stage (while it was still active further north in the belt) as the result of the drawing-off by thrusting of these formations from the internal zone onto a southern block (the Congo craton). Hence, the Yaounde Group is allochthonous. The recent highlighting by Nkoumbou et al. (2006) of ophiolite affinity rocks near Boumnyebel (west of the Yaoundé town) also support the thrust tectonics of the Yaoundé group onto the Ntem craton, although any real suture is not yet evidenced. To better access the allochthonous character of the Yaounde Group overlying the Congo craton, it is instructive to compare the results obtained in this study with data from the metasediments of the Mintom area (Fig.1c), where field relationships between different rock units are clearly revealed (IRGM, 2008). This area consists

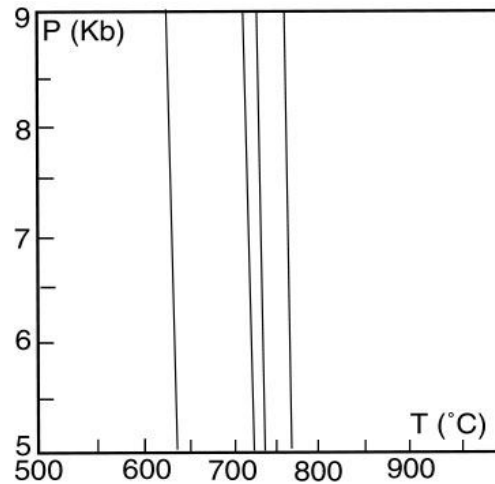


Fig. 8: Temperature curves derived by Garnet - Biotite geothermometer after Hodges and Spear, (1982).

of (Fig. 9a): (i) weakly deformed jaspers, red shales and conglomeratic sandstones representing the post-tectonic sedimentary cover and lying horizontally and unconformably over the metasedimentary cover and the Ntem complex (Congo craton); (ii) dolomites, limestones and low-grade schists (Mbalmayo series) representing the metasedimentary cover and lying

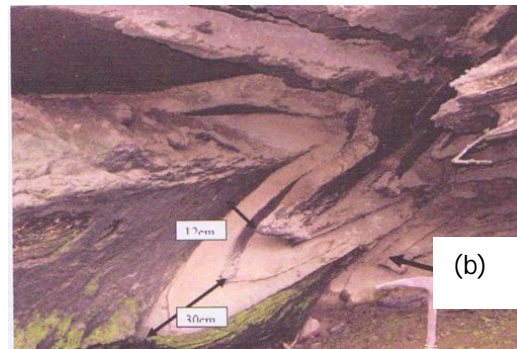
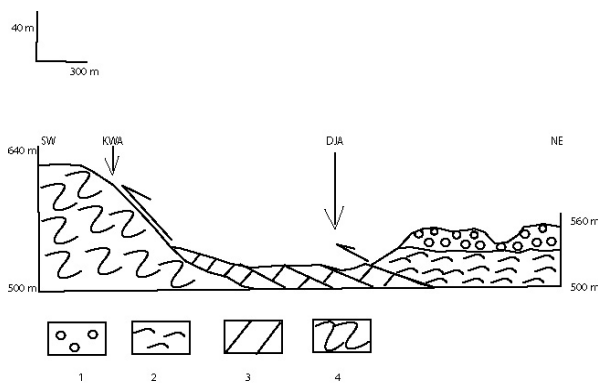


Fig. 9: (a) Interpretative cross section displaying the stratigraphy of the Mintom limestones; 1: weakly deformed jaspers, red shales and conglomeratic sandstones; 2: low grade schists (Mbalmayo schists); 3: deformed and slightly metamorphosed limestones and dolomites; Archean crust (Congo craton); (b) Photograph of synmetamorphic folded limestones; outcropview.

unconformably over the Ntem complex. Limestones are structurally overlain by schists and both rock units suffered a southward nappe thrust tectonic variously indicated by several structural features (e. g. flat lying foliation with an E-W strike and shallow dip ($< 20^\circ$) to the N; south vergent asymmetrical folding; Fig. 9b). The Ntem complex displays a rough sub-vertical foliation (N60°E/50), sheared by flat-lying ductile shear bands (of N50°E/30N direction) with a top to the south sense of movement. Hence, the metasediments of the Mintom area, at the edge of the Congo craton, appears to represent a small segment of the Yaounde Group, which was involved in thrust tectonics similar to the D_2 - D_3 events of the Yaounde Group in the Awaë-Ayos area.

5.0 CONCLUSION

The petro-structural analysis of the Yaounde Group in the Awaë-Ayos area indicates four main tectonic phases (D_1 , D_2 , D_3 and D_4). From the available data, the investigated area is interpreted as a folded pile of large scale allochthonous sheets, thrust to the West and the South-West over the Congo craton during the D_2 and D_3 Pan-African events. The metamorphic conditions grade from incipient metamorphism over the edge of the craton (sole of the nappe) to the granulite facies to the north (higher 9 kb and 750°C). The D_4 deformation corresponds to strike-slip shear zones after the completion of the nappe movement, contemporaneous with medium to low grade metamorphism; exhumation probably took place during this phase. The similarity in structural style between the Awaë-Ayos rocks and those from the metasediments of Mintom allows considering all these formations as a single allochthonous structural and metamorphic group thrust onto the Congo Craton during the Pan-African event.

Finally, from available data, a model is proposed, which could explain several features observed in the Yaounde Group such as: (i) compressive syn- D_2 and D_3 structures; (ii) the thickening of the crust and the subsequent HT - HP conditions; (iii) newly formed mineral associations close to the sole thrusts, defined by retrogressive phyllonites; (iv) the decompressional P-T path. In this model the dominant E-W to NE-SW - trending structures are the result of collisions and crustal thickening between three major continental domains involving the West African and Congo cratons, which squeezed reworked polycyclic domain during the Pan-African event; the expressions of this collisional stage are west- to south-west-directed allochthonous nappes

and thrust slices accompanied by folding on all scales (D_2). This stage is followed by southward compression (D_3) responsible for the dextral wrenching (D_4) after the completion of the nappe movement; we could therefore interpret some of these steep shear zones as lateral ramps of the Pan-African nappes thrust onto the Congo craton. Metamorphic isograds show a reverse metamorphism in the allochthonous slab identical to the classical Himalayan-type metamorphism (Lefort, 1975).

ACKNOWLEDGEMENTS

Thanks are given to Pr. Dr. Wolfgang Frisch and anonymous reviewers for their valuable comments. A thankful acknowledgement is made to the DAAD for its financial support.

REFERENCES

- Ball, E., Bard, J. P., Soba, D.** (1984). Tectonique tangentielle dans la catazone du Cameroun. Les gneiss de Yaoundé. *Journ. Afr. Earth Sci.* 2, 91-95.
- Berthé, D., Choukroune P., Jegouzo P.** (1979). Orthogneiss, Mylonite and non coaxial deformation of granite: The example of the south Armorican shear zone (France). *Journ. Struct. Geol.* 1, 31-42.
- Bohlen, S. R.** (1987). Pressure - temperature - time path and a tectonic model for the evolution of granulites. *Journ. Geol.* 95, 617 - 633.
- Champetier de Ribes, G., Aubague, M.** (1956). Carte géologique de reconnaissance du Cameroun à 1/500000, feuille Yaoundé - Est avec notice explicative. Direction des mines et de la géologie du Cameroun, 35 p.
- Dymek, R. F.** (1983). Titanium, aluminium and interlayered cation substitution in biotite from high-grade gneisses, west Greenland. *American Mineralogist.* 68, 880-889.
- Ferry, J. M., Spear, F. S.** (1978). Experimental calibration of the partitioning of Fe and Mg between biotite and garnet. *Contrib. to Mineral. and Petrol.* 66, 113-117.
- Ganguly, J., Saxena, S. K.** (1984). Mixing properties of aluminosilicate garnet: constraints from natural and experimental data, and applications to geothermobarometry. *Am. Mineral.* 69, 88-97.
- Hodges, K. V., Spear, F. S.** (1982). Geothermometry, geobarometry and Al₂SiO₅ triple point at Mt

Moosilauke, New Hampshire. *Am. Mineralogist* 67, 1118-1134

Indares, A., Martignole, J. (1985a). Biotite-garnet geothermometry in the granulite-facies rocks: The influence of Ti and Al in biotite. *Am. Mineral.* 70, 272-278.

Indares, A., Martignole, J. (1985 b). Biotite-garnet geothermometry in the granulite-facies rocks: evaluation of equilibrium criteria. *Can. Mineral.* 70, 272-278.

Institut de Recherches Géologiques et Minières (2008). Prospection géologique des calcaires de Mintom, Sud-Est Cameroun. Rapport de mission N°1, 27 p.

Jégouzo, P. (1984). Evolution structurale du Sud-Ouest Cameroun durant l'orogénèse panafricaine. Association tectoniques cisailante et chevauchante. Colloque CNRS, chevauchement et déformation, Toulouse: p. 23.

Kretz, R., (1983). Symbols for rock-forming minerals. *Am. Mineralogist* 68, 277-279

Lasserre, M., Soba, D. (1979). Migmatization d'âge panafricain au sein des formations camerounaises appartenant à la zone mobile de l'Afrique centrale. *C. R. Somm. Soc. Géol. France* 2, 64-68.

Lefort, P. (1975). Himalayas: The collided range. Present Knowledge of the continental arc. *American Journal of Science* 275-A, 1-44.

Manguelle Dicoum, E., Bokosah, A. S., Kwende Mbamwi, T. E. (1992). Geophysical evidence for a major Precambrian schist-granite boundary in Southern Cameroon. *Tectonophysics* 205, 437-446.

Maurizot, P. (1986). Carte géologique du Sud-Ouest Cameroun à 1/500000. Bureau de Recherches Géologiques et Minières. Orléans, France.

Mpesse, J. E., (1999). Etude pétrostructurale des formations métamorphiques de la région de Yaoundé et définition de la géométrie de sa tectonique tangentielle. Thèse, Doctorat de 3e cycle Univ. de Yaoundé I. 148p.

Mvondo, H. (2003). Analyse structurale et pétrogéochimique des roches de la région de Yaoundé nord. Arguments contribuant à la connaissance de l'évolution géotectonique de la chaîne panafricaine au Cameroun. Thèse Doctorat / Ph. D. Univ., Yaoundé I, 180 p.

Mvondo, H., den Brok, S. W. J., Mvondo Ondo, J. (2003). Evidence for symmetric extension and exhumation of the Yaoundé nappe (Pan-African fold belt, Cameroon). *Journ. Afr. Earth Sci.* 36, 215 - 213

Mvondo, H., Owona, S., Mvondo Ondo, J., Essono, J., (2007a). Tectonic evolution of the Yaoundé segment of the Neoproterozoic Central African Orogenic Belt in southern Cameroon. *Can. Journ of Earth Sci.* 44, 433-444.

Mvondo, H., Essono, J., Mvondo Ondo, J., Yene Atangana, J. Q. (2007b). Comment on "U-Pb dating of plutonic rocks involved in the nappe tectonic in southern Cameroon: Consequence for the central African fold belt" by Toteu et al. (*Journal of African Earth Sciences* 44 (2006) 479-493). *Journ Afr. Earth Sci.* 28, 49 - 52.

Nédelec, A., Macaudière, J., Nzenti, J. P., Barbey, P. (1986). Evolution structurale et métamorphique des schistes de Mbalmayo (Cameroun). Implications sur la structure de la zone mobile panafricaine d'Afrique Centrale au contact du craton du Congo. *C. R. Acad Sci., Paris* 303, série II, 75-80

Ngako, V., Jégouzo, P., Nzenti, J. P. (1992). Champ de raccourcissement et cratonisation du Nord Cameroun du protérozoïque supérieur au paléozoïque moyen. *C. R. Acad Sci., Paris* 315, série II, 371-377.

Ngako, V., Affaton, P., Nnange, J. M., Njanko, Th. (2003). Pan-African tectonic evolution in Central and southern Cameroon: Transpression and transtension during sinistral shear movements. *Journ. Afr. Earth Sci.* 36, 207-214.

Ngnotué, T., Nzenti, J. P., Barbey, P., Tchoua, F. M. (2000). The Ntui-Bétamba high grade gneisses: a northward extension of the panafrican Yaoundé gneisses in Cameroon. *Journ. Afr. Earth Sci.* 31, 369-381.

Nkoumbou, C., Yonta Goune, C., Villiéras, F., Njopwouo, D., Yvon, J., Ekodeck, G. E., Tchoua, F. (2006). Discovery of ophiolite-related rocks in the Pan-African belt in Cameroon: Talc schists from Ngoung, Lamal Pougue, and Bibodi Lamal. *Comptes Rendus Geosciences*, Vol. 338, 16, 1167-1175

Nzenti, J. P. (1987). Prétrogenèse des migmatites de Yaoundé (Cameroun). Eléments pour un modèle géodynamique de la chaîne panafricaine Nord-Equatoriale. Thèse de Doctorat de l'Université de Nancy I, 147 p.

Nzenti, J. P., Barbey, P., Macaudière, J. and Soba, D. (1988). Origin and evolution of the late Precambrian high grade Yaounde gneisses (Cameroon). *Precambrian Res.* 38, 91-109

Olinga, J. B. (2003). Cadre géodynamique et évolution tectonométamorphique des ensembles cristallophylliens d'Awaé et d'Ayos (Sud-Cameroun). Thèse Doctorat / Ph. D. Univ. Yaoundé I, 156 p.

Penaye, J., Toteu, S. F., Van Schmus, W. R., Nzenti, J. P. (1993). U-Pb and Sm-Nd preliminary geochronologic data on Yaounde series, Cameroon: Re-interpretation of the granulitic rocks as the suture of the collision in "centrafrican" belt. *C. R. Acad. Sci., Paris* 317, série II, 789-794.

Penaye, J., Toteu, S. F., Tchameni, R., Van Schmus, W. R., Tchakounté, J., Ganwa, A., Minyem, D., Nsifa, E. N. (2004). The 2.1 Ga West Central African Belt in Cameroon: extension and evolution. *Journ Afr. Earth Sci.* 39, 159-164.

Perchuk, L. L., Lavrent' Eva, I. V. (1983). Experimental investigations of exchange equilibria in the system cordierite-garnet-biotite. In: Saxena, S. K. (ed.), *Kinetics and equilibrium in mineral reactions*: Springer, Berlin, Heidelberg, New-York, pp. 199-239.

Spear, F. S. (1993). Metamorphic Phase Equilibria and Pressure - Time paths. *Mineralogical Society of America Monograph*, 1-799.

Thompson, A. B., Algor, J. R. (1977). Model systems for anatexis of politic rocks: I. theory of melting reactions the system $KAlO_2 - NaAlO_2 - Al_2O_3 - SiO_2 - H_2O$. *Contrib. Min. and petrol.* 63, 247 -269.

Toteu, S. F., Michard, A., Bertrand, J. M., Rocci, G., (1987). U/Pb dating of Precambrian rocks from Northern Cameroon, orogenic evolution and chronology of the Pan-African belt of Central Africa. *Precamb. Res.* 37, 71 - 87.

Toteu, S. F., Van Schmus, W. R., Penaye, J., Nyobe, J. B. (1994). U-Pb an Sm-Nd Evidence for Eburnian and Pan-African high-grade metamorphism in cratonic rocks of southern Cameroon. *Precamb. Res.* 67, 321-347.

Toteu, S. F.; Penaye, J.; Deloule, E.; Van Schmus, W. R.; Tchameni, R.; (2006). Diachronous evolution of volcano-sedimentary basins north of the Congo craton: Insights from U-Pb ion microprobe dating of zircon from the Poli, Lom and Yaoundé Groups (Cameroon). *Journ. Afr. Earth Sci.* 44, 428 - 442.

Received: 10/06/09

Accepted: 28/04/10